

## LETTER TO THE EDITOR

# Empirical estimate of Ly $\alpha$ escape fraction in a statistical sample of Ly $\alpha$ emitters

H. Atek<sup>1</sup>, D. Kunth<sup>1</sup>, D. Schaerer<sup>2,3</sup>, M. Hayes<sup>2</sup>, J. M. Deharveng<sup>4</sup>, G. Östlin<sup>5</sup>, J. M. Mas-Hesse<sup>6</sup><sup>1</sup> Institut d'Astrophysique de Paris (IAP), 98bis boulevard Arago, 75014 Paris, France<sup>2</sup> Observatoire de Genève, Université de Genève, 51 Ch. des Maillettes, 1290 Sauverny, Switzerland<sup>3</sup> Laboratoire d'Astrophysique de Toulouse-Tarbes, Université de Toulouse, CNRS, 14 Avenue E. Belin, 31400 Toulouse, France<sup>4</sup> Laboratoire d'Astrophysique de Marseille, UMR 6110 CNRS/Université de Provence, BP 8, Traverse du Siphon, 13376 Marseille Cedex 12, France<sup>5</sup> Oskar Klein Center for Cosmoparticle physics, Department of Astronomy, Stockholm University, 10691 Stockholm, Sweden<sup>6</sup> Centro de Astrobiología (CSIC-INTA), E28850 Torrejón de Ardoz, Madrid, Spain

Received date; accepted date

## ABSTRACT

**Context.** The Lyman-alpha (Ly $\alpha$ ) recombination line is a fundamental tool for galaxy evolution studies and modern observational cosmology. However, subsequent interpretations are still prone to a number of uncertainties. Besides numerical efforts, empirical data are urgently needed.

**Aims.** We empirically estimate the Ly $\alpha$  escape fraction in a statistically significant sample of  $z \sim 0$ –0.3 galaxies in order to calibrate high-redshift Ly $\alpha$  observations.

**Methods.** An optical spectroscopic follow-up of a sub-sample of 24 Ly $\alpha$  emitters detected by GALEX at  $z \sim 0.2$ –0.3, combined with a UV-optical sample of local starbursts, both with matched apertures, allow us to quantify the dust extinction through Balmer lines, and to estimate the Ly $\alpha$  escape fraction from the H $\alpha$  flux corrected for extinction and the recombination theory.

**Results.** The global escape fraction of Ly $\alpha$  radiation spans nearly the entire range of values, from 0.5 to 100 %, and  $f_{esc}(\text{Ly}\alpha)$  clearly decreases with increasing nebular dust extinction E(B-V). Several objects show  $f_{esc}(\text{Ly}\alpha)$  greater than  $f_{esc}(\text{continuum})$  which may be an observational evidence for clumpy ISM geometry, or for an aspherical ISM. Selection biases and aperture size effects may still exist between  $z \sim 0.2$ –0.3 Lyman-alpha emitters (LAEs) and local starbursts, which may explain the difference observed for  $f_{esc}(\text{Ly}\alpha)$ .

**Key words.** Galaxies: starburst – Galaxies: ISM – Ultraviolet: galaxies – ISM: extinction

## 1. Introduction

Considerable progress has been made in the last years in the detection and characterization of distant galaxy population. The advent of 8–10m class telescopes with large field of view (FOV) instruments allowed the conduction of very efficient surveys. In this context, the Ly $\alpha$  emission line is of particular interest since it proves the brightest spectral signature of remote young galaxies (Partridge & Peebles 1967; Schaerer 2003). High-redshift galaxies are now showing-up *en masse* thanks to the Lyman Break selection or emission line surveys (eg. Gronwall et al. 2007; Ouchi et al. 2008; Nilsson et al. 2008, and references therein), and the situation is likely to improve with upcoming Extremely Large Telescopes (ELTs) and the JWST. A comparable survey is now available for the first time at low redshift ( $z \sim 0.2$  – 0.35, Deharveng et al. 2008) thanks to GALEX (Galaxy Evolution Explorer) UV capabilities.

The Ly $\alpha$  line proves an invaluable tool in a cosmological context and gives rise to a wide variety of applications. Yet, in order to ensure a proper interpretation of the very promising Ly $\alpha$ -oriented studies, one has first to establish robust calibration on the basis of the complex transport of this line. The determination of the amount of Ly $\alpha$  radiation that escapes from the host starburst is probably the most important step toward understanding how various physical parameters may distort these Ly $\alpha$  interpretations. It is now well known that the escape of Ly $\alpha$  pho-

tons is affected by different physical processes: resonant scattering by neutral hydrogen and dust destruction (Neufeld 1990; Charlot & Fall 1993), velocity fields of the ISM (Lequeux et al. 1995; Kunth et al. 1998), multi-phase ISM (Neufeld 1991; Giavalisco et al. 1996; Hansen & Peng Oh 2006), underlying stellar absorption (Valls-Gabaud 1993), and star formation duty cycles (Valls-Gabaud 1993; Malhotra & Rhoads 2002). Although, the order of importance of these parameters begins to become clearer (e.g. Verhamme et al. 2008; Schaerer & Verhamme 2008; Atek et al. 2009b), a definitive empirical evidence, in a larger sample of galaxies, is still missing.

From the International Ultraviolet Explorer (IUE) to the Hubble Space Telescope (HST) era, spectroscopic and imaging observations of nearby star forming galaxies have played a key role in identifying the parameters responsible for the Ly $\alpha$  escape complexity. Recent high resolution Ly $\alpha$  imaging results clearly demonstrate the importance of resonant scattering, showing locally very high Ly $\alpha$ /H $\alpha$  ratios and a large Ly $\alpha$  scattering halo (e.g. Hayes et al. 2007; Atek et al. 2008; Östlin et al. 2008). However, most results obtained so far have no statistical bearing and are still difficult to generalize because the sample is rather small and consists of specific “hand-picked” objects. We propose here to rectify this by using a sample of 24 Ly $\alpha$  emitting galaxies at  $0.2 \lesssim z \lesssim 0.35$  found by GALEX. We have carried out a spectroscopic follow-up of a southern sub-sample with EFOSC2 on the ESO New Technology Telescope (NTT). This enables us

to analyze how the Ly $\alpha$  emission is related to the physical properties of galaxies. We also re-analyzed UV-optical spectra of a sample of 11 local starbursts. For the first time, these large aperture observations allow us to determine empirically the Ly $\alpha$  escape fraction in a large sample of galaxies, and to examine its dependence on dust extinction if any.

## 2. Observations

### 2.1. The GALEX sample

96 Ly $\alpha$  emitting galaxies at  $z \sim 0.2$ –0.35 were found by Deharveng et al. (2008) in the GALEX spectroscopic survey. The observations (available in the GALEX GR2 data release) made use of the far ultraviolet (FUV, 1350 $\text{\AA}$  – 1750 $\text{\AA}$ ) and near ultraviolet (NUV, 1950 $\text{\AA}$  – 2750 $\text{\AA}$ ) for a slitless blind search for Ly $\alpha$  emitters. Five fields with a total area of 5.65 deg $^2$  were used to extract all spectra of point sources with a minimum signal-to-noise ratio (S/N) per resolution element of 2 in the FUV and 3 in the NUV. Galaxies are then visually selected on the basis of potential Ly $\alpha$  emission feature, which naturally lead to a threshold of  $EW_{\text{Ly}\alpha} \gtrsim 10\text{\AA}$ . Characteristics of data reduction and the five fields used are described in more details in Deharveng et al. (2008).

### 2.2. Spectroscopic follow-up

Spectroscopic observations of 24 of the 31 galaxies in the Chandra Deep Field South (CDFS) and ELAIS-S1 fields were undertaken with EFOSC2 on the NTT at ESO La Silla. Two instrumental setups were used: (1) spectrophotometric mode with a 5'' slit, which allows us to encompass the whole galaxy and (2) spectroscopic mode with a 1'' slit, which gives a better spectral resolution to correct H $\alpha$  for N $\text{II}$  contamination. Both settings were used in combination with Grism #13 covering a large wavelength range in the optical domain (3690–9320 $\text{\AA}$ ), giving access to lines from [O $\text{II}$ ] 3727 $\text{\AA}$  to [S $\text{II}$ ] 6717+6731  $\text{\AA}$  at this redshift range. A binning of  $2 \times 2$  is used corresponding to a plate-scale of 0.24'' px $^{-1}$  and a spectral resolution of FWHM  $\sim 12\text{\AA}$  (for 1'' slit spectra). To avoid second order contamination that affects the grism used here, an order sorting filter is mounted to cut off light blue-ward  $\sim 4200\text{\AA}$ . Observational settings and exposure times are summarized in Table 1.

**Table 1.** NTT EFOSC2 observations

Mode	Slit	Tot Exp(s)	Nb Obj	Grism
Spectroscopy	1''	4600	24	13
Spectrophotometry	5''	2000	20	13

The EFOSC2 spectra were reduced and calibrated using standard IRAF routines. The aperture extraction of 1D spectra is performed through the DOSLIT task where the dispersion solution is obtained from internal lamp calibration spectra to correct for telescope position variations. Finally, spectra were flux calibrated using a mean sensitivity function determined from standard stars observations from Oke (1990) catalog.

### 2.3. IUE starburst sample

We re-analyzed UV-optical spectra of 11 local starburst galaxies, presented in McQuade et al. (1995) and Storchi-Bergmann et al. (1995); and sufficiently distant to separate the geocoronal Ly $\alpha$  emission. Data consist of *IUE* UV (1200–3300  $\text{\AA}$ ) spectra combined with ground-based optical spectra with matched aperture (20''  $\times$  10''). In most cases, there is a good agreement between the UV red-end and the optical blue-end of the spectra; otherwise, the optical spectrum is rescaled to match the UV one. For more details, see the above-cited publications. Furthermore, we included in our analysis only net Ly $\alpha$  emitters, i.e. with  $EW_{\text{Ly}\alpha} > 0$ . The line measurements are performed following the same procedure used for the NTT spectra.

### 2.4. Emission line measurements

The spectra were analyzed using the SPLIT package in IRAF. The redshifts of the galaxies were measured by visual inspection of good S/N lines, and line measurements performed interactively on rest-frame spectra. For all our objects, we confirm, with a better accuracy, the redshift determination by the Ly $\alpha$  selection. The identification of the Ly $\alpha$  feature on the grism mode of *GALEX* proves a posteriori very robust.

Fluxes and equivalent widths (EWs) are measured, when available, for [O $\text{II}$ ] 3727 $\text{\AA}$ , [O $\text{III}$ ] 4959, 5007  $\text{\AA}$ , H $\delta$ , H $\gamma$ , H $\alpha$ , H $\beta$  and [N $\text{II}$ ] 6548, 6584  $\text{\AA}$ . For most spectra, the H $\alpha$  line (6563  $\text{\AA}$ ) is blended with [N $\text{II}$ ] lines (6548 and 6584  $\text{\AA}$ ) even for the 1'' slit observations. In this case a deblending routine is used within SPLIT to measure individual fluxes in each line. Then, N $\text{II}$ /H $\alpha$  line ratio is used to correct the spectrophotometric observations for [N $\text{II}$ ] contamination. To correct for underlying stellar absorption in the Balmer lines we assume a constant equivalent width of 2  $\text{\AA}$ , typical of starburst galaxies (Tresse et al. 1996; González Delgado et al. 1999).

To determine uncertainties in the line fluxes we run 1000 Monte Carlo simulations in which random Gaussian noise, based on the data noise, is added to a noise-free spectrum, and the emission lines are then fitted. The MC errors computed depend essentially on the S/N quality of spectra. Error propagation is applied through the calculation of all the quantities described above and the line ratios, extinction etc. computed hereafter.

Using BPT diagrams (Baldwin et al. 1981; Veilleux & Osterbrock 1987), and *Chandra* X-ray observations, we have identified at most three galaxies possibly excited by an active galactic nucleus (AGN), which represents up to 12.5 % of our sample. This diagnostic is thoroughly addressed in Atek et al. (2009a).

### 2.5. Extinction

Reddening along the galaxy line of sight is caused by interstellar dust extinction. The reddening contribution of our Galaxy is negligible, since all our objects are located at high galactic latitude. Then the extinction coefficient,  $C(H\beta)$ , intrinsic to the observed object can be calculated using the Balmer ratio between H $\alpha$  and H $\beta$ :

$$\frac{f(H\alpha)}{f(H\beta)} = R \times 10^{-C[S(H\alpha)-S(H\beta)]}, \quad (1)$$

where  $f(H\alpha)$  and  $f(H\beta)$  are the measured integrated fluxes and  $R$  is the intrinsic Balmer ratio. We use here a value of  $R = 2.86$ , assuming case B recombination theory and a temperature of  $10^4$  K (Osterbrock 1989). Using the Seaton (1979) extinction law,

we have  $S(H\alpha) - S(H\beta) = -0.323$ . The colour excess  $E_{B-V}$  is then simply computed using Eq. 1 and the relation  $E(B-V) = C/1.47$ . For objects that have a negative extinction within the uncertainties, we set their value to zero.

### 3. Ly $\alpha$ escape fraction

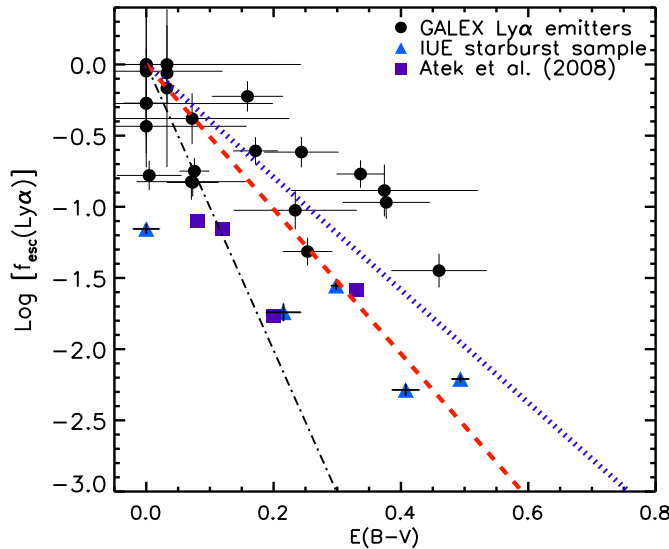


**Fig. 1.** Ly $\alpha$  escape fraction as a function of dust extinction, observed in  $z \sim 0.3$  Ly $\alpha$  galaxies. The red dashed line is the best fit to all the observations (GALEX, IUE, and Atek et al. samples). The dark dot-dashed line represent the best fit determined by Verhamme et al. (2008) from spectral fitting of  $z \sim 3$  LBGs. The blue dotted line corresponds to the escape fraction of the continuum attenuated by dust extinction using Seaton (1979) law (see text for details).

To determine the intrinsic Ly $\alpha$  flux, and subsequently the Ly $\alpha$  escape fraction we follow Atek et al. (2008). The method relies on the fact that H $\alpha$  emission is not prone to complex radiation transport effects and is only affected by dust attenuation. Therefore correcting the observed H $\alpha$  flux for extinction and assuming a case B recombination theory (Osterbrock 1989), one can estimate the intrinsic Ly $\alpha$  flux. The Ly $\alpha$  escape fraction is then given by:

$$f_{\text{esc}}(\text{Ly}\alpha) = f(\text{Ly}\alpha)/(8.7 \times f(\text{H}\alpha)_C), \quad (2)$$

where  $f(\text{Ly}\alpha)$  is the observed flux and  $f(\text{H}\alpha)_C$  is the extinction-corrected H $\alpha$  flux.

Figure 1 shows our empirical  $f_{\text{esc}}$  values as a function of the nebular extinction for the GALEX and IUE samples described above. Also shown are  $f_{\text{esc}}$  values for 4 nearby galaxies with  $EW_{\text{Ly}\alpha} > 0$  Å determined by Atek et al. (2008) from HST imaging. This figure actually summarizes many information with several implications on Ly $\alpha$  physics.

First, we find that  $f_{\text{esc}}$  is anything but constant, but spans a wide range of values, typically from  $f_{\text{esc}} \sim 0.5$  to 100 % in the GALEX sample. Second, the Ly $\alpha$  escape fraction is clearly sensitive to the dust extinction and an anti-correlation is observed. The red dashed curve is the best fit to the observations corresponding to

$$f_{\text{esc}}(\text{Ly}\alpha) = 10^{-0.4 k(\text{Ly}\alpha) E(B-V)} \quad \text{with } k(\text{Ly}\alpha) \sim 12.7 \quad (3)$$

The parameter  $k(\text{Ly}\alpha)$  correspond to a new Ly $\alpha$  extinction coefficient derived from our fit, and differs from the classical one at Ly $\alpha$  wavelength  $k(1216)$ . It takes into account the averaged effects of all processes affecting the Ly $\alpha$  escape, such as the resonant scattering experienced by Ly $\alpha$  photons, which increases their mean path and therefore the effective dust optical depth, or velocity fields in the gas or the ISM geometry, which may ease the escape of Ly $\alpha$ . The observed scatter around our mean relation is most likely indicative of this multi-parameter process. For similar extinctions, the Ly $\alpha$  escape fraction seems to be higher on average in GALEX Ly $\alpha$  galaxies than in local objects. In the  $z \sim 0$  objects,  $f_{\text{esc}}$  never exceed  $\sim 10\%$ , whereas at  $z \sim 0.3$  it covers a wide range of values as high as 100%. This difference may be the result of different selection effects. The GALEX galaxies are selected from their Ly $\alpha$  emission amongst spectra issued from a blind search, whereas the local objects are from a sample of starburst galaxies selected from the optical.

Third, several objects show  $f_{\text{esc}}(\text{Ly}\alpha)$  greater than the escape fraction expected for the continuum near Ly $\alpha$  (blue dotted line) corresponding to  $f_{\text{esc}}(\text{cont}) = 10^{-0.4 k(1216) E(B-V)}$ , where the most favourable value  $k(1216) \sim 9.9$  is adopted here from the Seaton law. Although Ly $\alpha$ /H $\alpha$  ratios exceeding the theoretical value have already been found in local starbursts (Atek et al. 2008), this was only the case locally in spatially resolved objects, where this can easily be explained by a local Ly $\alpha$  “excess” due to scattering. Here, the “global” Ly $\alpha$  escape fraction determined from the integrated spectra is found to be higher than expected from the most favourable (i.e. flattest) attenuation law in some objects. These objects may be observational evidence for a multi-phase configuration of the ISM (Neufeld 1991; Hansen & Peng Oh 2006), where dust is primarily distributed in cold neutral clouds with a ionized inter-clouds medium. By reflecting on the clouds surface, Ly $\alpha$  photons will be easily transmitted through the ionized medium. Approximately 2/6 of these objects show also a relatively high Ly $\alpha$  equivalent width ( $EW_{\text{Ly}\alpha} \sim 100-150$  Å), as may be expected for a clumpy ISM. Alternatively a Ly $\alpha$  escape fraction higher than the UV continuum could also be due to orientation effects in objects with an aspherical ISM, e.g. in conical outflows into which Ly $\alpha$  would be “channeled” more effectively than continuum radiation. The Ly $\alpha$  escape fraction of objects below the attenuation curve of the continuum ( $f_{\text{esc}}(\text{Ly}\alpha) \lesssim f_{\text{esc}}(\text{cont})$ ) can be understood quantitatively by models with a homogeneous ISM, as shown in Fig. 2. However, this does not exclude that clumping may also play a role in these objects.

On Fig. 2, we have plotted for comparison, the results of an extensive grid of 3D Ly $\alpha$  radiation transfer simulations in homogeneous, spherically expanding shells (Hayes et al. 2009b) using an updated version of the MC $\text{Ly}\alpha$  code (Verhamme et al. 2006). Also plotted are the fits/trends already shown in Fig. 1. Here the model E(B-V) is computed from the predicted UV continuum attenuation, and assuming the same extinction law as above. The large variation of the predicted  $f_{\text{esc}}$  values is mostly due to variations in the expansion velocity of the shell, its H $\alpha$  column density, and the Doppler parameter  $b$ . As clearly seen from this figure, the present model grid covers the bulk of the observed variations in  $f_{\text{esc}}$  and E(B-V). The homogeneous, spherical shell models may thus in principle be able to explain the majority of the objects, although tailored models including all observational constraints need to be done to confirm this. However, the  $f_{\text{esc}}$  values above the continuum attenuation curve (blue dotted line) observed in 6 objects, cannot be explained with these models, since Ly $\alpha$  photons cannot be less attenuated than the continuum in a homogeneous ISM. Approximately 2/6 of these objects

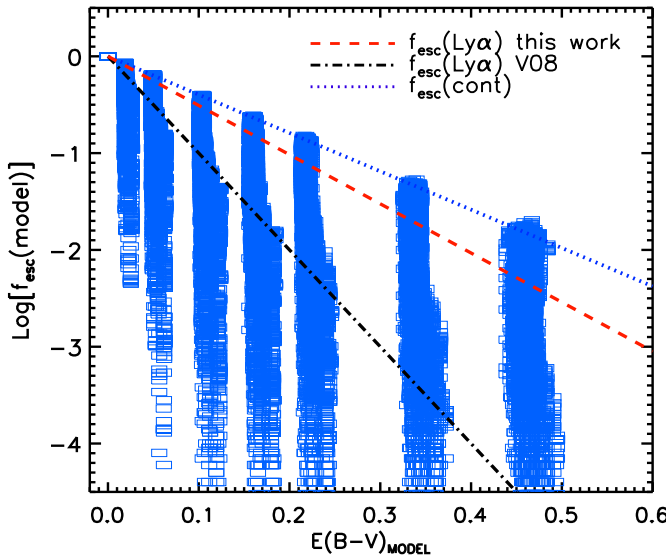


**Fig. 2.** Predictions for  $f_{esc}(\text{Ly}\alpha)$  using a 3D Ly $\alpha$  radiation transfer code (Verhamme et al. 2006). The dark curve is the best fit for modeled  $z \sim 3$  LBGs (Verhamme et al. 2008) and the blue rectangles (forming columns) are the predicted values of  $f_{esc}(\text{Ly}\alpha)$  versus  $E(B - V)$  (Hayes et al. 2009b) using all combinations of the remaining parameters ( $v_{exp}$ ,  $N(\text{H}\text{i})$ ,  $b$  ...). The two remaining curves are the same as in Fig. 1.

show also a relatively high Ly $\alpha$  equivalent width ( $EW_{\text{Ly}\alpha} \sim 100$ –150 Å), as may be expected for a clumpy ISM. New radiation transfer computations in clumpy media are underway to examine this interesting behaviour.

#### 4. Discussion

We have presented here an estimation of the mean Ly $\alpha$  escape fraction as a function of the extinction and how different parameters can alter this simple relation. We have carefully chosen our aperture (5'' slit) in optical spectroscopy in order to get Balmer fluxes comparable to Ly $\alpha$  one obtained by *GALEX* grism. This allow us to estimate the extinction and the escape fraction for the whole galaxy as it is the case for slitless spectroscopy of *GALEX* observations. Indeed, it appears that the dust extinction is sensitive to the aperture size, since our 1'' slit observations, targeting the center of the galaxies, lead in general to a higher extinction.

For the sake of coherence between the different samples, we decided to minimize selection effects by retaining only the net Ly $\alpha$  emitters in the *IUE* and imaging samples. We recall that the *IUE* local starbursts retained are all aperture matched between ground-based optical spectroscopy and *IUE* large aperture (20''  $\times$  10'') UV observations. Furthermore, there is no aperture size concerns for the Ly $\alpha$  imaging objects. However, while the slitless mode of *GALEX* enables us to recover the entire diffuse Ly $\alpha$  emission, to deal with comparable Ly $\alpha$  and Balmer fluxes, this is not necessarily the case for *IUE* observations. The size of the large aperture may remain for some nearby objects insufficient to encompass the scattered photons across a large area of the galaxy, as usually indicated by the large extent of the H $\text{i}$  gas. Therefore,  $f_{esc}(\text{Ly}\alpha)$  could be slightly underestimated. On the contrary, as mentioned earlier, the  $z \sim 0.2$ –0.3 objects are selected on the grounds of their Ly $\alpha$  strength. This will likely favor the high Ly $\alpha$  escape fractions. One should then keep in mind these opposite effects that contribute to stretch the deviation

from our best fit of this compilation of data points. Similar Ly $\alpha$  equivalent width criteria are commonly applied to select high- $z$  LAEs, implying most likely relatively high escape fractions and a less severe discrepancy between Ly $\alpha$  and non-resonant radiation for this class of objects. A blind search of Ly $\alpha$  emitters would then unveil lower  $f_{esc}(\text{Ly}\alpha)$  than the *GALEX* objects. That is the case for our current double blind survey in Ly $\alpha$  and H $\alpha$  at  $z \sim 2.2$ , where we find an average escape fraction of  $\sim 4\%$  (Hayes et al. 2009a).

In contrast with other emission lines, the dust extinction is only one of several parameters governing  $f_{esc}(\text{Ly}\alpha)$ , and the extent of the dispersion around the fit is a good illustration. Given the importance of an accurate estimation of  $f_{esc}(\text{Ly}\alpha)$  one need to quantify the kinematical effects by measuring the cold ISM velocity in these objects. An additional step toward a precise calibration of  $f_{esc}(\text{Ly}\alpha)$ . A more detailed investigation of the physical properties, and SED modeling of our sample will be the scope of subsequent publications (Atek et al. 2009a).

*Acknowledgements.* We thank Daniela Calzetti, who kindly put her UV-optical spectra of the IUE sample at our disposal. The work of DS and MH is supported by the Swiss National Science Foundation. HA and DK are supported by the Centre National d'Etudes Spatiales (CNES). GÖ is Royal Swedish Academy of Sciences Research Fellow supported by a grant from the Knut and Alice Wallenberg Foundation. GÖ acknowledges support from the Swedish research council. This work is based on observations made with ESO Telescopes at La Silla Observatories under programme ID 082.B-0392.

#### References

Atek, H., Kunth, D., Hayes, M., Östlin, G., & Mas-Hesse, J. M. 2008, A&A, 488, 491  
 Atek, H., Kunth, D., Schaerer, D., et al. 2009a, A&A, *in preparation*  
 Atek, H., Schaerer, D., & Kunth, D. 2009b, ArXiv e-prints  
 Baldwin, J. A., Phillips, M. M., & Terlevich, R. 1981, PASP, 93, 5  
 Charlot, S. & Fall, S. M. 1993, ApJ, 415, 580  
 Deharveng, J.-M., Small, T., Barlow, T. A., et al. 2008, ApJ, 680, 1072  
 Giavalisco, M., Koratkar, A., & Calzetti, D. 1996, ApJ, 466, 831  
 González Delgado, R. M., Leitherer, C., & Heckman, T. M. 1999, ApJS, 125, 489  
 Gronwall, C., Ciardullo, R., Hickey, T., et al. 2007, ApJ, 667, 79  
 Hansen, M. & Peng Oh, S. 2006, New Astronomy Review, 50, 58  
 Hayes, M., Östlin, G., Atek, H., et al. 2007, MNRAS, 382, 1465  
 Hayes, M., Östlin, G., Schaerer, D., & Verhamme, A. 2009a, A&A, *in preparation*  
 Hayes, M., Schaerer, D., & Verhamme, A. 2009b, A&A, *in preparation*  
 Kunth, D., Mas-Hesse, J. M., Terlevich, E., et al. 1998, A&A, 334, 11  
 Lequeux, J., Kunth, D., Mas-Hesse, J. M., & Sargent, W. L. W. 1995, A&A, 301, 18  
 Malhotra, S. & Rhoads, J. E. 2002, ApJ, 565, L71  
 McQuade, K., Calzetti, D., & Kinney, A. L. 1995, ApJS, 97, 331  
 Neufeld, D. A. 1990, ApJ, 350, 216  
 Neufeld, D. A. 1991, ApJ, 370, L85  
 Nilsson, K. K., Tapken, C., Moeller, P., et al. 2008, ArXiv e-prints  
 Oke, J. B. 1990, AJ, 99, 1621  
 Osterbrock, D. E. 1989, Astrophysics of gaseous nebulae and active galactic nuclei (Research supported by the University of California, John Simon Guggenheim Memorial Foundation, University of Minnesota, et al. Mill Valley, CA, University Science Books, 1989, 422 p.)  
 Östlin, G., Hayes, M., Kunth, D., et al. 2008, ArXiv e-prints  
 Ouchi, M., Shimasaku, K., Akiyama, M., et al. 2008, ApJS, 176, 301  
 Partridge, R. B. & Peebles, P. J. E. 1967, ApJ, 147, 868  
 Schaerer, D. 2003, A&A, 397, 527  
 Schaerer, D. & Verhamme, A. 2008, A&A, 480, 369  
 Seaton, M. J. 1979, MNRAS, 187, 73P  
 Storchi-Bergmann, T., Kinney, A. L., & Challis, P. 1995, ApJS, 98, 103  
 Tresse, L., Rola, C., Hammer, F., et al. 1996, MNRAS, 281, 847  
 Valls-Gabaud, D. 1993, ApJ, 419, 7  
 Veilleux, S. & Osterbrock, D. E. 1987, ApJS, 63, 295  
 Verhamme, A., Schaerer, D., Atek, H., & Tapken, C. 2008, ArXiv e-prints, 805  
 Verhamme, A., Schaerer, D., & Maselli, A. 2006, A&A, 460, 397